This is the accepted manuscript made available via CHORUS. The article has been published as:

Observation of Phase-Filling Singularities in the Optical Dielectric Function of Highly Doped n-Type Ge

Chi Xu, Nalin S. Fernando, Stefan Zollner, John Kouvetakis, and José Menéndez

Phys. Rev. Lett. **118**, 267402 — Published 27 June 2017

DOI: 10.1103/PhysRevLett.118.267402

Observation of phase-filling singularities in the optical dielectric function of highly doped *n*-type Ge

Chi Xu[1], Nalin S. Fernando[2], Stefan Zollner[2], John Kouvetakis[3], and José Menéndez[1]

[1]Department of Physics, Arizona State University, Tempe, AZ 85287-1504, USA

[2]Department of Physics, New Mexico State University, Las Cruces, NM 88003-8001, USA

[3]School of Molecular Sciences, Arizona State University, Tempe, AZ 85287-1604, USA

Phase-filling singularities in the optical response function of highly-doped ($> 10^{19}$ cm^{-3}) germanium are theoretically predicted and experimentally confirmed using spectroscopic ellipsometry. Contrary to direct-gap semiconductors, which display the well-known Burstein-Moss phenomenology upon doping, the critical point in the joint-density of electronic states associated with the partially filled conduction band in *n*-Ge corresponds to the so-called E_1 and $E_1+\Delta_1$ transitions, which are two-dimensional in character. As a result of this reduced dimensionality, there is no edge shift induced by Pauli blocking. Instead, one observes the "original" critical point (shifted only by band gap renormalization) and an additional feature associated with the level occupation discontinuity at the Fermi level. The experimental observation of this feature is made possible by the recent development of low-temperature, *in situ* doping techniques that allow the fabrication of highly doped films with exceptionally flat doping profiles.

Van Hove critical point singularities in the valence-conduction joint density of states (JDOS) manifest themselves as sharp features in the complex optical dielectric function $\varepsilon(E)$ of crystalline solids.[1] Additional structure arises in metallic systems due to the abrupt change in the occupation number at the Fermi level E_F.[2] Similar phase-filling singularities are in principle expected in highly-doped semiconductors. However, most semiconductor studies so far have focused on direct gap E_0 transitions involving a three-dimensional (3D) maximum in the valence band and a 3D minimum in the conduction band, which give rise to a 3D minimum in the JDOS. For this M_0 critical point, which corresponds to the fundamental band gap in many III-V and II-VI compounds, Pauli blocking suppresses transitions involving states between the band edge and E_F, so that only transitions to states beyond E_F contribute to the dielectric function. Experimentally, this means that a single critical point feature is expected at an energy that increases monotonically as a function of doping. This phenomenology is usually described as a Burstein-Moss "shift" [3,4]. The observation of *separate* band-structure and phase-filling singularities has not been reported for doped semiconductors. The essential requirement for their observation is a lower-dimensionality JDOS critical point structure associated with the band extrema. A prototypical candidate is Ge, for which the so-called E_1 and $E_1+\Delta_1$ transitions involving the bottom of the conduction band are two-dimensional in character. However, in spite of studies spanning several decades [5-8], no clear experimental evidence for a phase-filling singularity has emerged for Ge or for any other material with a similar band structure. Part of the reason is that the high donor levels needed to observe the effect are usually achieved by implantation/recrystallization methods. The structural quality of such material is clearly inferior to that of pristine Ge, and the doping profiles are hardly uniform. This smears out the singularities and makes it difficult to differentiate between optical effects induced by doping and those related to the introduction of defects. Very recently, however, there has been a revival of interest in *n*-type Ge as possible laser gain medium, and this has led to the development of new *in situ* doping methods [9-13] that preserve the crystal quality and make it possible to obtain extremely flat doping profiles. In this letter we report the observation of phase filling singularities in such *in situ*-doped *n*-type Ge films.

The experimental accessibility of phase filling singularities clearly separated from band-structure singularities could provide new impetus to studies of many-body effects at the Fermi level, a subject of great current interest. [14-20]. Furthermore, the observations reported here are

not necessarily limited to the peculiar band structure of doped-Ge. Materials that have attracted recent theoretical attention due to their possible non-trivial topological properties, such as GaBi and InBi[21], and perhaps even α-Sn [22], are predicted to have occupied states similar to those of doped Ge, so that the spectroscopic approach reported here may contribute to unraveling their intriguing electronic structure.

All doped Ge samples were grown on *i*-Ge-buffered Si substrates produced in a gas source molecular epitaxy (GSME) reactor using Ge_4H_{10} at around 350°C [23]. P doped samples with $n < 4\times10^{19}$ cm^{-3} were grown in the same reactor using mixtures of Ge_4H_{10} and $P(GeH_3)_3$. Highly doped samples ($n \geq 4\times10^{19}$ cm^{-3}) were grown in a hot-wall CVD reactor at 330-340°C using mixtures of Ge_3H_8 and $P(GeH_3)_3$ or SbD_3. Typical *n*-layer thicknesses were 200 nm. Secondary ion mass spectroscopy (SIMS) measurements revealed flat dopant profiles and sharp transitions at the *n/i* interfaces. Doping levels were determined by infrared ellipsometry, Hall, and SIMS measurements. Carrier concentrations determined by all methods agree well, and all samples showed almost full dopant activation.[24]

The $\varepsilon(E)$ function was determined using two JA Woollam™ UV-Vis variable angle spectroscopic ellipsometers. Low-temperature measurements were conducted at an incident angle of 70° and energy steps of either 0.005 eV or 0.010 eV. Room temperature measurements were usually conducted at a 0.005 eV step size for 3 different incidental angles (65°, 70° and 75°) The measurements yield the ellipsometric angles $\Psi(E)$ and $\Delta(E)$, and these are described using a multiple-layer model that incorporates the substrate, the buffer layer, a thin transition layer between buffer and doped film, the doped film itself, and a roughened (~1-2 nm) GeO_2 layer at the surface. The function $\varepsilon(E)$ for the doped film was first adjusted to the data using a parametric model (Ref. [25]). For this fit the dielectric function for the remaining layers were taken from ellipsometer manufacturer's database. In the case of GeO_2 we used data from Hu *et al*. [26]. The adjustable parameters of the fit are the layer thicknesses and all constants in the parametric model for the doped layer. In a subsequent fit stage, we keep the thicknesses from the initial fit and fit again the dielectric function of the doped layer, this time without assuming any theoretical model but using the real (ε_1) and imaginary (ε_2) parts of the $\varepsilon(E)$ at each energy as adjustable parameters. The resulting fit values are used as seed parameters for the next energy values, and by following this "point-by-point" procedure, $\varepsilon(E)$ is obtained over the entire energy range.

Second and higher derivatives of $\varepsilon(E)$ make it possible to isolate the contributions from critical points. Due to the unavoidable presence of noise, however, numerical filters must be used for data differentiation. The Savitzky-Golay (S-G) method[27-29] is an excellent option because it removes noise while preserving the lineshape of narrow features. For this work, however, we found that a regularization method, [30], produces somewhat better results. We minimize an objective function that contains a term proportional to the square of the fourth derivative of the data times a weighting parameter λ, so that for λ=0 one recovers the original data. We use the largest possible value of λ (typically $\lambda(\Delta E)^{-8} = 10^{18}$, where ΔE is the energy step) for which the lineshape of the main features of the numerical second derivative matches the lineshape obtained under S-G differentiation. For such value of λ, the noise is visibly reduced relative to the S-G case.

Figure 1 shows the relevant portions of the Ge band structure calculated using the $k\cdot p$ method of Ref. [31]. In n-type Ge, electrons accumulate in the conduction band that has minimum at $L = \frac{\pi}{a_0}(1,1,1)$, where a_0 is the cubic lattice constant. This minimum is clearly 3D but highly anisotropic, with a longitudinal effective mass of $1.58m$ (left panel) and transverse effective mass of $0.083m$ (right panel) [32]. The top valence band right below this conduction band runs very parallel to the above conduction band for a distance $k_{\max} \sim \pi/a_0$ along the [111] direction (measured from the L point), giving rise to a critical point in the JDOS that manifests itself as the sharp E_1 structures in the dielectric function of Ge at E_1 = 2.2 eV. For all realistic levels of doping, the Fermi vector k_F along the [111] direction (measured from the L point), satisfies $k_F < k_{\max}$, so that Pauli blocking will suppress some but not all transitions at energy E_1. This is a crucial difference with the total suppression of transitions

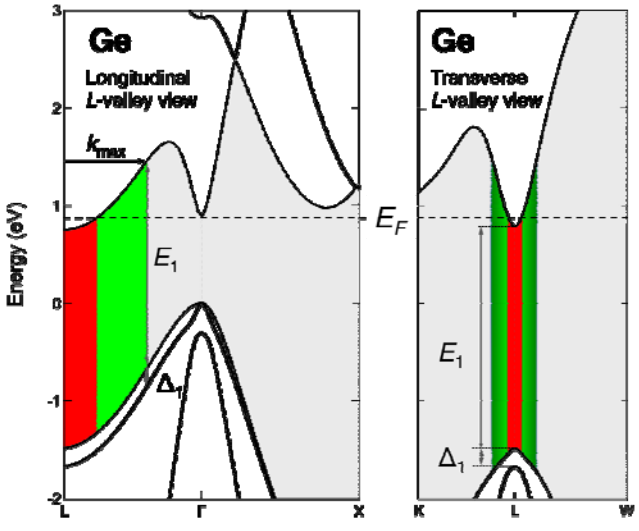

Figure 1. Band structure of Ge calculated with the $k\cdot p$ method of Ref. 31, highlighting the region corresponding to the E_1 and $E_1+\Delta_1$ transitions. For the E_1 case, we show schematically the effect of Pauli blocking following n-type doping. Red indicates forbidden transitions at $T = 0$. Green shows allowed transitions at $T = 0$. Darker greens correspond to higher energies.

at the gap energy E_0 in direct gap semiconductors such as GaAs.

Since the conduction and valence bands run parallel from $k = L$ to $k = k_{max}$, the critical point can be approximated as a two-dimensional (2D) minimum. Its contribution to ε_2 was given by Cardona [33]. For the case of *n*-type Ge, the expression can be generalized[34][35] to

$$\varepsilon_2(E) = \frac{8e^2\overline{P}^2\mu_\perp}{3m^2E^2} H(E-E_1) \int_{-k_{max}}^{k_{max}} dk_z \left\{1 - f\left[E_c\left(E,k_z^2\right)\right]\right\} \tag{1}$$

In Eq. (1) $\overline{P}^2$ is the square of the average momentum matrix element and $\mu_\perp$ is the transverse reduced electron-hole mass. A value $\overline{P}^2/m$ = 12.9 eV reproduces the experimental value of $m_\perp$ using ***k·p*** theory [33]. At the same level of theory one obtains $\mu_\perp^{-1} = \left(\overline{P}^2/m^2\right)\left[2/E_1 + 1/\left(E_1+\Delta_1\right)\right]$ for the E_1 gap and $\mu_\perp^{-1} = \left(\overline{P}^2/m^2\right)\left[1/E_1 + 2/\left(E_1+\Delta_1\right)\right]$ for the E_1+Δ_1 gap. $H(x)$ In Eq. (1) is the Heaviside step function, and $f(E)$ the Fermi function, whose argument is given by

$$E_c\left(E,k_z^2\right) = \frac{\hbar^2k_z^2}{2m_\parallel} + \left(E-E_1\right)\frac{\mu_\perp}{m_\perp} \tag{2}$$

if E_F is measured from the bottom of the conduction band. At a temperature $T = 0$, Eq. (1) gives

$$\varepsilon_2(E) = \frac{16e^2\overline{P}^2\mu_\perp}{3m^2E^2} H(E-E_1)k_{max} \times$$
$$\times \begin{cases} 1 & \text{for } E > E_1 + \dfrac{m_\perp}{\mu_\perp}E_F \\ 1 - \dfrac{1}{k_{max}}\sqrt{\dfrac{2m_\parallel}{\hbar^2}\left[E_F - \left(E-E_1\right)\dfrac{\mu_\perp}{m_\perp}\right]} & \text{for } E < E_1 + \dfrac{m_\perp}{\mu_\perp}E_F \end{cases} \tag{3}$$

This function is plotted in Figure 2(e), and we see that Pauli blocking "removes" the upper corner of $\varepsilon_2(E)$, thereby creating a new singularity at $E = E_1 + \left(m_\perp/\mu_\perp\right)E_F$. At non-zero temperatures the integral in Eq. (1) can be performed numerically, and the phase-filling singularity is found to be broadened by the smearing of the Fermi function, as shown in Fig. 2(f) for T = 77 K. In this panel we have also applied the experimental broadening of the E_1 transition at the same temperature.[36,37] The second derivative of ε_2 is shown in Fig. 2(g), with a clear feature (highlighted with an arrow) associated with the phase-filling singularity. The contribution of the E_1 transition to the real part ε_1 of the dielectric function can be obtained from the imaginary part by utilizing the Kramers-Kronig (K-K) relations. The real part of ε_1 at a given

energy E contains contributions from optical transitions over the entire spectral range. However, only those transitions around E contribute sharp features near E, so that the second derivative of the K-K transform of Eq. (3) should be comparable to the second derivative of the ε_1 obtained as a K-K transform of the entire $\varepsilon_2(E)$. The K-K transform of Eq. (3) is shown in Fig. 2(a). The corresponding calculation for T = 77 K appears in Fig. 2(b), and Fig. 2(c) shows the second derivative, with a clear feature corresponding to the phase-filling singularity, highlighted by an arrow.

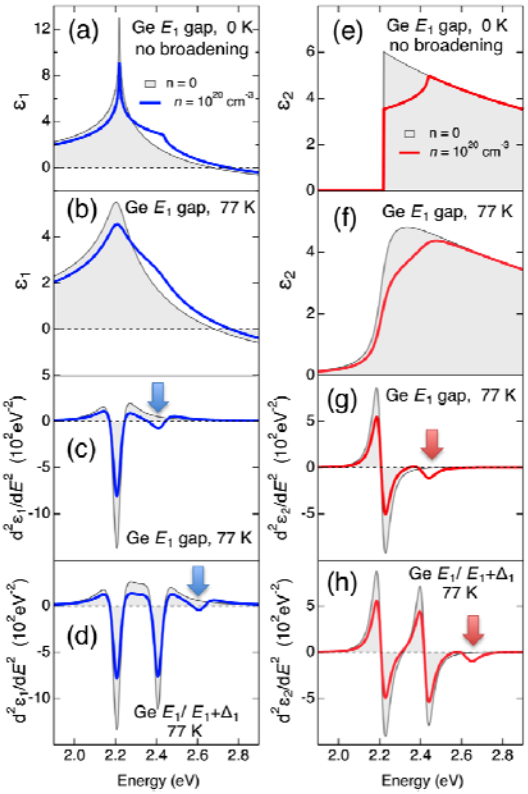

Figure 2 Calculated real (blue) and imaginary (red) parts of the dielectric function and their second derivatives near the E_1 /E_1+Δ_1 gaps of intrinsic and doped Ge. The top three panels (a-c) and (e-g) on each side only show the E_1 contribution to better illustrate the effect of doping. The bottom panels (d) and (h) incorporate the full E_1/E_1+Δ_1 for comparison with experiment. The arrows mark the position of the extra features due to doping. In all cases, the grey curves correspond to the undoped case.

The experimental observation of doping effects on $\varepsilon(E)$ is not as straightforward as in the above discussion due to the presence, next to the E_1 critical point, of a second critical point associated with the E_1+Δ_1 transition between the second valence band in Fig. 1 and the conduction band. The E_1+Δ_1 contribution to $\varepsilon_2(E)$ is given by an expression identical to Eq. (1), but since E_1+Δ_1 appears at higher energies than E_1, it overlaps with the Fermi-level feature associated with the E_1 transition that we calculated in Fig. 2. Figs 2(d) and 2(h) show the calculated second derivatives including both transitions. The phase-filling feature corresponding to the E_1 transition manifests itself as subtle changes in the lineshape of the E_1+Δ_1 contribution, and only the phase-filling features associated with the E_1+Δ_1 transition are easy to observe, as indicated by the arrows. An additional complication is that in the undoped case Eq. (1) gives a poor description of the experimental dielectric function because it does not include excitonic effects. These are usually accounted for by multiplying Eq. (1) times an amplitude A and by additionally incorporating a phase factor $\exp(i\phi)$ in the expression for the complex dielectric function, which effectively mixes real and imaginary parts.

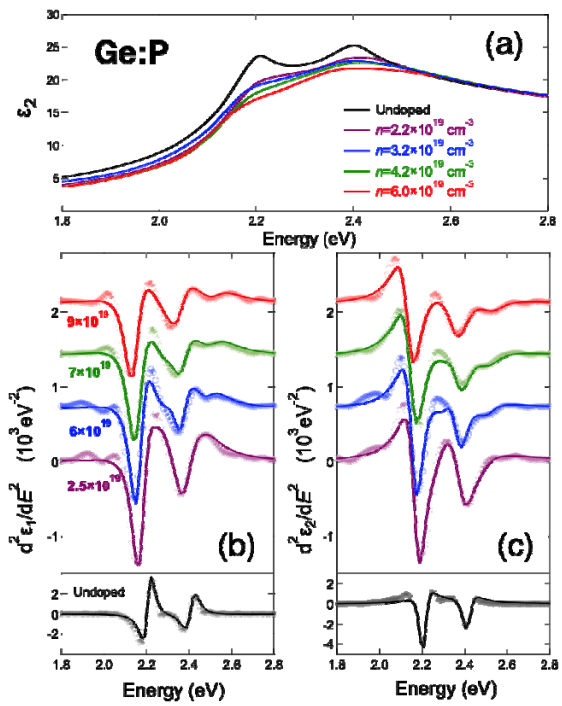

Figure 3 (a) Imaginary part of the 77K dielectric function for several *n*-type Ge films. The lower panels show second derivatives of the complex dielectric function of the above films. The solid lines represent simultaneous fits of the real and imaginary parts with an expression derived from Eq. (1). Traces are vertically offset by 700 eV^{-2} each for clarity. (b) Real parts. The doping levels that produce the best fit are indicated below the corresponding traces. (b) Imaginary parts.

Figure 3(a) shows the imaginary part ε_2 of the dielectric function for films with different levels of P doping. As predicted in Figs. 2(e-f) we see a monotonic overall decrease in ε_2 as a result of Pauli blocking. Furthermore, whereas in pure Ge ε_2 decreases rapidly at energies above the two critical points, we observe an increase in the doped samples, also as predicted in Figs. 2(e-f). In analogy with our treatment of the model calculation, we can gain more insight into the doping effects by computing second derivatives of the experimental dielectric function. The results are in panels (b) and (c). We notice the appearance of a feature in both the real and imaginary parts that is very similar to the predicted phase-filling singularity, as shown in Figs. 2(d) and 2(h). To make the connection between theory and experiment more quantitative we carried out a fit of the experimental data using expressions based on Eq. (1). We first calculate the Fermi level corresponding to the dopant concentration in our sample using a model that includes not only the *L* valley but also the Γ and *X* valleys. The value of E_F is then inserted into Eq. (1) to obtain the E_1 and $E_1+\Delta_1$ contributions to ε_2. To simulate lifetime broadening effects, $\varepsilon_2(E)$ is convoluted with a Lorentzian. The $\varepsilon_1(E)$ function is obtained from a K-K transform. For this model the adjustable parameters of the fit are therefore the energy, Lorentzian width Γ and the amplitude parameters *A* for the E_1 and $E_1+\Delta_1$ transitions, plus a common phase angle ϕ. The fits are repeated for different values of the dopant concentration until a best fit is found. These are indicated below the real part traces in Fig. 3(a). The numbers in parenthesis below are the carrier concentrations measured by IR ellipsometry.

The agreement with theory is quite remarkable. We are able to predict the energy position of the phase-filling singularity in both the real and imaginary parts using carrier concentrations within a factor of 2 of the experimental values. Furthermore, we also reproduce the temperature dependence of the feature.[23] Even in the case of the lowest doped sample ($n = 2.5 \times 10^{19}$ cm^{-3}) in which no separate peak is observed, we see an additional broadening of the $E_1+\Delta_1$ structure that indicates the presence of the Fermi level feature. In this context it is interesting to note that the earlier data from Ref. [7] also show a distinct additional broadening of the $E_1+\Delta_1$ transition relative to E_1 transition in a highly doped sample. Our results suggest that this apparent extra broadening is caused by the merger of the $E_1+\Delta_1$ transition and phase-filling feature. Our theory predicts no Burstein-Moss upshifts for *n*-type Ge, and in fact we observe a *downshift* of up to 0.18 eV in the energies of the E_1 and $E_1+\Delta_1$ main transitions, which is due to band gap renormalization upon doping [38]. A full account of renormalization effects will be published elsewhere.

The phase factors that give the best fit of the data are quite large. For pure Ge, we obtain $\phi = 105°$, as evidenced by the very different lineshapes in Fig. 3 and Fig. 2 (the latter corresponds to $\phi = 0°$) The phase angle decreases monotonically as a function of the doping concentration, as previously observed [7]. For the highest-doped sample in Fig. 3 we obtain $\phi = 35°$. The smaller phase angle manifests itself as a better agreement between the measured lineshapes and the predictions from Fig. 2. This is consistent with the screening of the excitonic interaction by the free carriers. The phase factor might be further reduced by computing the dielectric function directly from the band structure, rather than from a model density of states, but this would drastically increase the complexity of the fit. Fortunately, we note that in Fig. 2 the phase-filling features have a similar lineshape in the real and imaginary parts, so that these features are rather insensitive to the mixing induced by a phase factor. The amplitude A remains near 2-3 for all samples, which means that the ε_2 reduction in Fig 3, is entirely accounted for by Pauli blocking. The values of A are consistent with the excitonic enhancements observed at other transitions, but the reason why they do not decrease as a function of doping is unclear, particularly in view of the observed decrease in ϕ . This behavior could indicate the need for a more refined treatment of broadening, or it could be viewed as evidence for additional excitonic effects in doped systems, such as the so-called Mahan exciton, which should be a subject of further studies.[39]

In summary, we have predicted and observed phase-filling singularities in the dielectric function of highly doped *n*-type Ge films. The experimental data are satisfactorily explained with an expression that accounts for Pauli blocking. These results provide sensitive information on the conduction band of *n*-type Ge and open up a new spectroscopic tool to study carrier-exciton interactions in heavily doped systems.

The ASU work was supported by the Air Force Office of Scientific Research under contracts DOD AFOSR FA9550-12-1-0208 and AFOSR FA9550-13-1-0022, and by the National Science Foundation (NSF) under grant DMR-1309090. The work at NMSU was supported by AFOSR FA9550-13-1-0022NSF and by NSF under grant DMR-1505172.

REFERENCES

[1] P. Y. Yu and M. Cardona, *Fundamentals of Semiconductors: Physics and Materials Properties* (Springer-Verlag, Berlin, 1996).
[2] C. Y. Fong, M. L. Cohen, R. R. L. Zucca, J. Stokes, and Y. R. Shen, Phys. Rev. Lett. **25**, 1486 (1970).
[3] E. Burstein, Phys. Rev. **93**, 632 (1954).
[4] T. S. Moss, Proceedings of the Physical Society. Section B **67**, 775 (1954).
[5] J. Humlíček, phys. stat. sol. (b) **86**, 303 (1978).
[6] A. K. Sood, G. Contreras, and M. Cardona, Phys. Rev. B **31**, 3760 (1985).
[7] L. Viña and M. Cardona, Phys. Rev. B **34**, 2586 (1986).
[8] S. Prucnal *et al.*, Sci Rep **6**, 27643 (2016).
[9] G. Scappucci, G. Capellini, W. C. T. Lee, and M. Y. Simmons, Appl. Phys. Lett. **94**, 162106 (2009).
[10] R. E. Camacho-Aguilera, Y. Cai, J. T. Bessette, L. C. Kimerling, and J. Michel, Optical Materials Express **2**, 1462 (2012).
[11] C. Xu, C. L. Senaratne, J. Kouvetakis, and J. Menéndez, Appl. Phys. Lett. **105**, 232103 (2014).
[12] C. Xu, J. D. Gallagher, P. M. Wallace, C. L. Senaratne, P. Sims, J. Menéndez, and J. Kouvetakis, Semicond. Sci. Technol. **30**, 105028 (2015).
[13] C. Xu, C. L. Senaratne, J. Kouvetakis, and J. Menéndez, Phys. Rev. B **93**, 041201 (2016).
[14] S. Schmitt-Rink, D. S. Chemla, and D. A. B. Miller, Adv. Phys. **38**, 89 (1989).
[15] F. Fuchs, K. Kheng, P. Koidl, and K. Schwarz, Phys. Rev. B **48**, 7884 (1993).
[16] T. Makino, K. Tamura, C. H. Chia, Y. Segawa, M. Kawasaki, A. Ohtomo, and H. Koinuma, Phys. Rev. B **65**, 121201 (2002).
[17] M. Feneberg, J. Däubler, K. Thonke, R. Sauer, P. Schley, and R. Goldhahn, Phys. Rev. B **77**, 245207 (2008).

[18] M. A. Versteegh, D. Vanmaekelbergh, and J. I. Dijkhuis, Phys Rev Lett **108**, 157402 (2012).
[19] M. Feneberg *et al.*, Phys. Rev. B **90**, 075203 (2014).
[20] M. Feneberg, J. Nixdorf, C. Lidig, R. Goldhahn, Z. Galazka, O. Bierwagen, and J. S. Speck, Phys. Rev. B **93**, 045203 (2016).
[21] H. Huang, J. Liu, and W. Duan, Phys. Rev. B **90**, 195105 (2014).
[22] C. Hoffman, J. Meyer, R. Wagner, F. Bartoli, M. Engelhardt, and H. Höchst, Phys. Rev. B **40**, 11693 (1989).
[23] C. Xu, R. T. Beeler, L. Jiang, G. Grzybowski, A. V. G. Chizmeshya, J. Menéndez, and J. Kouvetakis, Semicond. Sci. Technol. **28**, 105001 (2013).
[24] See Supplemental Material at [URL] for sample characteristics, dielectric function curves, complete sets of fit parameters for second derivatives of the dielectric function, temperature dependencies, and details on the numerical second derivatives.
[25] B. Johs, C. M. Herzinger, J. H. Dinan, A. Cornfeld, and J. D. Benson, Thin Solid Films **313-314**, 137 (1998).
[26] Y. Z. Hu, J. T. Zettler, S. Chongsawangvirod, Y. Q. Wang, and E. A. Irene, Appl. Phys. Lett. **61**, 1098 (1992).
[27] A. Savitzky and M. J. E. Golay, Anal. Chem. **36**, 1627 (1964).
[28] J. Steiner, Y. Termonia, and J. Deltour, Anal. Chem. **44**, 1906 (1972).
[29] H. H. Madden, Anal. Chem. **50**, 1383 (1978).
[30] J. J. Stickel, Computers & Chemical Engineering **34**, 467 (2010).
[31] D. Rideau, M. Feraille, L. Ciampolini, M. Minondo, C. Tavernier, H. Jaouen, and A. Ghetti, Phys. Rev. B **74**, 195208 (2006).
[32] G. Dresselhaus, A. Kip, and C. Kittel, Phys. Rev. **98**, 368 (1955).
[33] M. Cardona, in *Atomic Structure and Properties of Solids*, edited by E. Burstein (Academic Press, New York, 1972), pp. 514.
[34] J. Humlíček and F. Lukeš, phys. stat. sol. (b) **77**, 731 (1976).
[35] We assume that in our n-type materials the valence band is fully occupied at any temperature, as corroborated by direct calculations of the equilibrium hole concentration p.
[36] L. Viña, S. Logothetidis, and M. Cardona, Phys. Rev. B **30**, 1979 (1984).
[37] N. S. Fernando *et al.*, Applied Surface Science (2016).
[38] S. C. Jain and D. J. Roulston, Solid-State Electronics **34**, 453 (1991).
[39] G. D. Mahan, Phys. Rev. **153**, 882 (1967).